



Robust detection of overlapping bioacoustic sound events

Louis Mahon^{1,2,†} Benjamin Hoffman^{1,†} Logan S James^{1,3} Maddie Cusimano¹ Masato Hagiwara¹ Sarah C Woolley³ Olivier Pietquin¹

¹Earth Species Project

²University of Edinburgh

³McGill University

[†]Equal Contribution

lmahonology@gmail.com, benjamin@earthspecies.org

Abstract

We propose a method for accurately detecting bioacoustic sound events that is robust to overlapping events, a common issue in domains such as ethology, ecology and conservation. While standard methods employ a frame-based, multi-label approach, we introduce an onset-based detection method which we name `Voxaboxen`. It takes inspiration from object detection methods in computer vision, but simultaneously takes advantage of recent advances in self-supervised audio encoders. For each time window, `Voxaboxen` predicts whether it contains the start of a vocalization and how long the vocalization is. It also does the same in reverse, predicting whether each window contains the end of a vocalization, and how long ago it started. The two resulting sets of bounding boxes are then fused using a graph-matching algorithm. We also release a new dataset designed to measure performance on detecting overlapping vocalizations. This consists of recordings of zebra finches annotated with temporally-strong labels and showing frequent overlaps. We test `Voxaboxen` on seven existing data sets and on our new data set. We compare `Voxaboxen` to natural baselines and existing sound event detection methods and demonstrate SotA results. Further experiments show that improvements are robust to frequent vocalization overlap.

1 Introduction

Detecting the sounds produced by animals is the foundation of bioacoustics research. This task must often be performed using noisy recordings that include many overlapping sounds from multiple individuals. Identifying each individual acoustic unit is necessary for a diversity of tasks, including species recognition and population estimation, which are critical to research on topics such as ecology and conservation Laiolo [2010], Odom et al. [2021], Penar et al. [2020].

Within a species, animals often produce overlapping sounds with important functional consequences Kershenbaum et al. [2016]. For example, large colonies of gregarious species such as zebra finches, penguins, and bats can be noisy, with near continuously overlapping vocalizations Aubin and Jouventin [2002], Elie et al. [2011], Zann [1996], Gillam and Fenton [2016]. Similarly, many species of frog chorus together, and the timing of call overlaps can have consequences for receiver responses, with some species even producing nearly synchronous calls Clulow et al. [2017], Fitzsimmons et al. [2008], Larter and Ryan [2024], Legett et al. [2019, 2021]. Overlapping sounds also occur in specific contexts within a group, such as elephant rumbles Soltis et al. [2005], wolf howls Harrington et al. [2003], and sperm whale clicks Schulz et al. [2008]. To understand these diverse communication systems, large-scale identification of individual vocalizations, including accurate classification of overlapping sounds, is of critical importance.

Motivated by this, we are interested in a sound event detection (SED) method that is able to predict the onset time, offset time, and class label (e.g., species label) for sound events that overlap. Commonly, SED methods adopt a frame-based multi-label classification approach: for each time frame, for each class of interest, the system makes a binary prediction of whether a sound of that class occurs in that frame Cakir et al. [2017], Shao et al. [2024], Martin et al. [2022], Ebbers et al. [2024]. When a given class occurs in consecutive frames, these frames are merged into a single event. Crucially, this does not accommodate situations that require detect overlapping vocalizations that share one class, such as a species label. While standard object detection methods from computer vision like Faster-RCNN Ren et al. [2016] or DETR Carion et al. [2020] can be adapted to perform SED and theoretically support overlapping

arXiv:2503.02389v1 [cs.SD] 4 Mar 2025

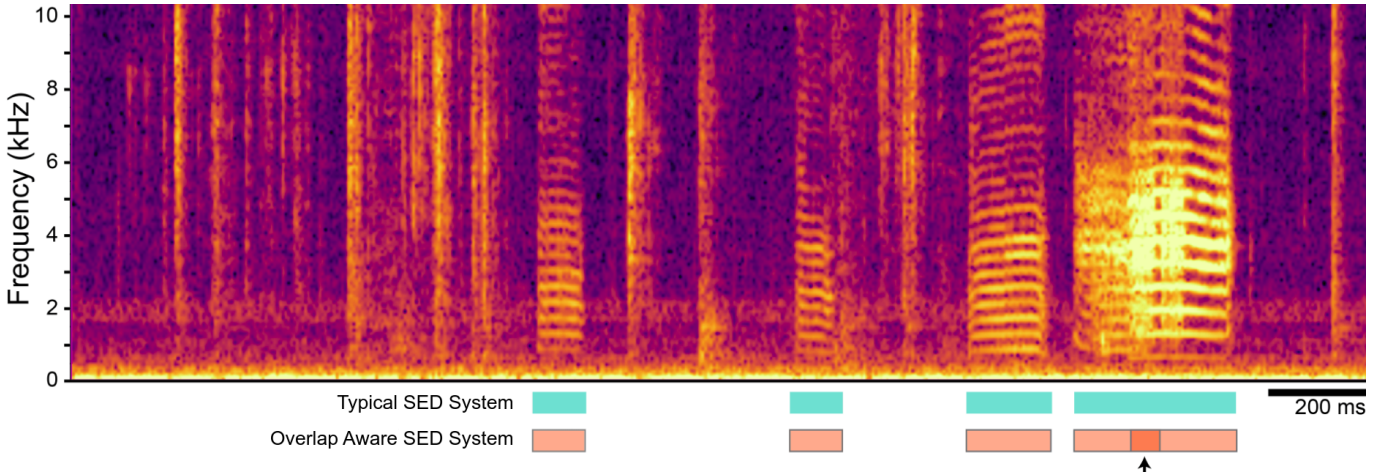


Figure 1: Example spectrogram from the dataset we release, containing five female zebra finch calls; two of these overlap as indicated by an arrow. Frame-based systems merge these final two calls into one event, but using *Voxaboxen* we are able to distinguish them

predictions, they fail to take advantage of recent advances in audio encoders trained with self supervised learning (SSL) Chen et al. [2023], Shao et al. [2024], Hagiwara [2023].

To address this limitation, we propose a method we name *Voxaboxen*, which employs pretrained SSL audio encoders but abandons the standard multi-label frame-based approach and instead detects the onset of sound events. Specifically, for each frame, *Voxaboxen* makes a binary prediction as to whether it contains the onset of an event, plus a regression prediction for how long that event will last, and a classification prediction (such as a species label). This design choice of predicting a label in $\{\text{onset, other}\}$ at each time step, rather than in $\{\text{vocalization, other}\}$ means the duration of one predicted event can extend past the onset of a second event, thus allowing the model to predict overlapping vocalizations without them being merged (see Figure 1).

To investigate how well *Voxaboxen* deals with overlapping vocalizations, we introduce a new dataset of recordings of eight female zebra finches (ZFs) spontaneously interacting in a laboratory environment. Our dataset includes manual annotations of the onset and offset of each vocalization, and features a high proportion of overlapping vocalizations. We evaluate *Voxaboxen* on our dataset, and find that it significantly outperforms existing methods. We also introduce a series of synthetic datasets, consisting of ZF vocalizations with a controlled overlap-to-vocalization ratio. We find that *Voxaboxen* consistently outperforms alternatives, even in the presence of a high degree of overlap. Additionally, in comparison to existing methods on seven additional datasets, we find that *Voxaboxen* significantly outperforms the alternatives, providing evidence that the SSL audio encoder affords a performance benefit.

Taken together, our results demonstrate the general effectiveness of *Voxaboxen* for bioacoustic SED, including for situations with overlapping vocalizations. To democratize putting boxes around vocalizations, we open source the code for our model and new dataset¹.

To summarize, the contributions of this paper are as follows: (1) highlighting the importance of detecting overlapping vocalizations, and how most existing transformer-based models cannot do this; (2) introducing a new SED model, *Voxaboxen*, which leverages SSL pretrained transformer features and can predict overlapping vocalizations; (3) releasing a new dataset, OZF, specifically focussed on overlapping vocalizations; (4) experimental evaluation on a diverse set of eight datasets, showing SotA performance for *Voxaboxen*.

2 Related Work

Sound event detection Standard approaches to SED make multi-label predictions for each frame of audio Cakir et al. [2017], Shao et al. [2024], which are merged to determine the onset and offset of each sound event. In bioacoustics applications, SED has also typically been framed as a multi-label classification problem Stowell [2022], with temporal resolution of predictions ranging from tens of milliseconds Cohen et al. [2022], Martin et al. [2022], to multiple seconds Kahl et al. [2021]. Recent post-processing techniques decouple event durations and detections Ebberts et al. [2024], Yoshinaga et al. [2025]; however these still operate on multi-label frame-based predictions and do not

¹Released upon publication

accommodate overlapping events that share a single label. Some methods have focused on the specific case that 3d directional coordinates are available, and proposed methods to separate sources by location Adavanne et al. [2018], Shimada et al. [2022]. Older methods have specifically targeted overlapping vocalizations Dessein et al. [2013], Bisot et al. [2017], but use matrix factorization algorithms rather than deep learning encoders.

Object detection methods from computer vision such as Faster-RCNN Ren et al. [2016] have occasionally been applied to SED Algabri et al. [2020], including in bioacoustics Zsebők et al. [2019]. CornerNet Law and Deng [2018] is an object detection method that, similar to `Voxaboxen`, matches predicted boundaries into a single event, but differs in that it has to predict both dimensions of the box and that it matches based on feature similarity, which is not suitable for detecting multiple overlapping boxes of the same class.

Source separation Given an audio recording with a mixture of sound sources, source separation is the task of predicting the audio of the un-mixed sounds. Prior work in bioacoustics has demonstrated the effectiveness of both supervised Bermant [2021] and unsupervised methods Denton et al. [2022] for improving accuracy in downstream classification tasks. In our context, a source separation model could theoretically separate vocalizations from multiple individuals into different audio tracks, thus reducing the complexity of the audio passed to a downstream detection model. We investigate this type of approach as an alternative to `Voxaboxen`.

Speaker diarization A related task to the one we focus on is speaker diarization. Given a recording of multiple (typically human) speakers, a speaker diarization model must detect (possibly overlapping) speech segments and assign each segment to a speaker. Approaches typically assume a maximum number of speakers (e.g., two or four), and make use of the assumption that speakers can be re-identified by their vocal characteristics across multiple segments Bredin and Laurent [2021] In contrast, we assume no maximum number of speakers, and do not expect to re-identify individuals within a recording. While animal speaker identification has recently seen some interest Martin et al. [2022], Stowell et al. [2019], current approaches rely on difficult-to-acquire ground-truth individual labels, and may struggle with individual identification across different taxa.

3 Method

3.1 Bounding Box Regression

Our method uses a frame-based audio encoder to produce a sequence of latent vectors (we used a fixed frame rate of 50 Hz, taken from the encoder). A final linear layer makes three types of predictions, for each time frame: a prediction of the probability that an event starts in that frame, a prediction of the duration of the event (should it start in that frame), and a prediction of a class label for the event (should it start in that frame) chosen from a predetermined ontology.

Using gradient descent, we minimize the loss function $L = L_{det} + \lambda L_{reg} + \rho L_{cls}$, $\lambda, \rho \geq 0$, which includes a detection term L_{det} , a regression term L_{reg} , and a classification term L_{cls} . The detection term is inspired by the penalty-reduced focal loss in Law and Deng [2018]:

$$L_{reg} = -\frac{1}{T} \sum_{t=1}^T \begin{cases} (1 - \hat{p}_t)^\alpha \log \hat{p}_t & p_t = 1 \\ (1 - p_t)^\beta \hat{p}_t^\alpha \log(1 - \hat{p}_t) & p_t < 1. \end{cases}$$

Here, T is the duration in frames of the audio clip, and α and β are hyperparameters. The model’s predicted detection probability at time t is \hat{p}_t , and the target p_t is obtained by smoothing each event onset with a Gaussian kernel and taking the per-frame maximum:

$$p_t = \max_{x \in \text{Events}} \exp\left(-\frac{(t - \text{Onset}(x))^2}{\text{Dur}(x)^2 / \sigma}\right).$$

In this equation, `Events` is the set of events in a audio clip, and for $x \in \text{Events}$, $\text{Onset}(x)$ and $\text{Dur}(x)$ denote the onset time and duration of x .

The regression term L_{reg} is L1 loss, applied only to frames in $\{\text{Onset}(x) \mid x \in \text{Events}\}$, i.e. frames where an event begins. Similarly, the classification term L_{cls} is a categorical cross-entropy loss, again applied only when an event begins. At inference time, we apply a peak-finding algorithm to the time-series of detection probabilities. Detection peaks above a threshold become boxes, with duration and class prediction determined by the value of the

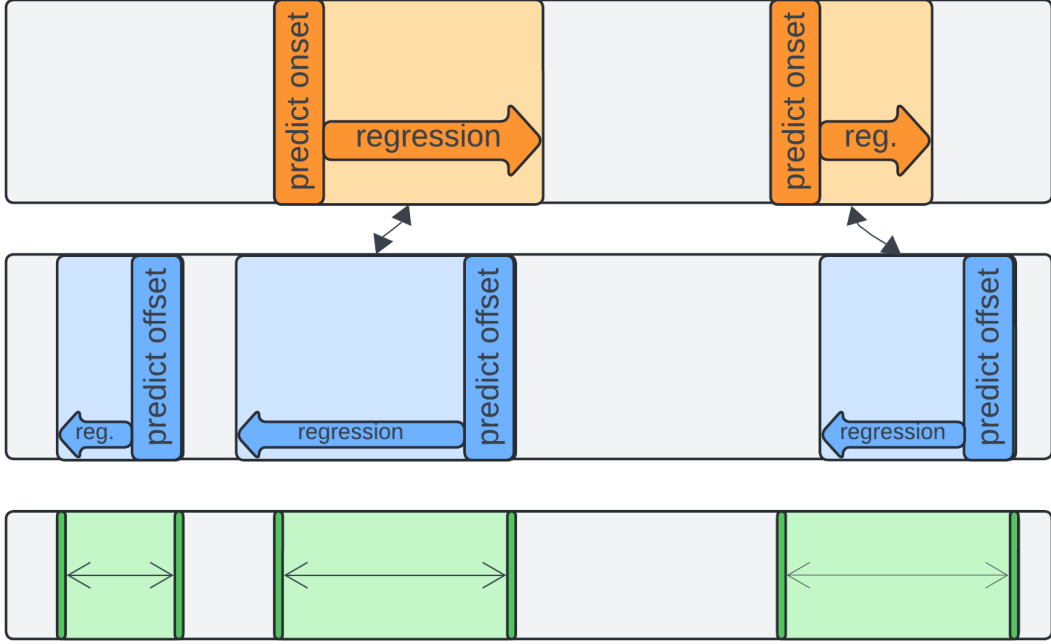


Figure 2: Example of our forward-backward matching. Top: 3 fwd predictions, from predicting onset and regressing forward. Middle: 3 bck predictions, from predicting offset and regressing back. Bottom: final output predictions, the 1st is the 1st bck prediction, the 2nd is the combination of the 1st fwd and 2nd back, the 3rd is the combination of the 2nd fwd and 3rd back. The matching is indicated with the black arrows. Combinations take the onset from the fwd prediction and the offset from the bck prediction.

regression and classification predictions at the peak. The detection threshold is swept (for computing some metrics), or fixed as a hyperparameter; see Section 5. Finally, we apply soft non-maximal suppression Bodla et al. [2017] to remove duplicate boxes.

3.2 Bidirectional Predictions

One drawback of using these predicted boxes directly is the difficulty for the model in making accurate regression predictions. In preliminary experiments, we observed that onset predictions tend to be more accurate than offset predictions, which may be due to the presence of local acoustic features that typically indicate the onset, versus a relative lack of such features to inform the future prediction of how long the event will last. Therefore, we make a second set of predictions which are the mirror image of the first: a binary prediction for each frame as to whether it contains an offset, plus a regression for how long the event lasted. We then compute an optimal way to fuse the forward and backward predictions, into a single set of predictions by casting the problem as a maximum graph matching. Our final predictions take the forward onset time and the backward offset time.

Formally, when predicting over a time interval of length T , and C possible classes, let F and B be the forward and backward predicted boxes, respectively, which are produced by the peak-finding step described in the previous section. Each box consists of the timestep it was predicted at (f_t, b_t) , the detection probability (f_d, b_d) , the regression value for its duration (f_r, b_r) , and the class probabilities (f_c, b_c) :

$$F = \left(f_t^i, f_d^i, f_r^i, f_c^i \right)_{1 \leq i \leq k}$$

$$B = \left(b_t^i, b_d^i, b_r^i, b_c^i \right)_{1 \leq i \leq l}$$

where, for each i , $f_t^i \in [0, T]$, $f_d^i \in [0, 1]$, $f_r^i \in \mathbb{R}^+$, $f_c^i \in \mathbb{R}^C$, and $i > j \Rightarrow f_t^i < f_t^j$, and similarly for B . Then define a weighted bipartite graph $G = (F \cup B, F \times B)$, where the weight function W is the intersection over union (IoU):

$$W((f_t, f_d, f_r, f_c), (b_t, b_d, b_r, b_c)) = \frac{\max(0, \min(f_t + f_r, b_t) - \max(f_t, b_t - b_r))}{\min(f_r + b_r, \max(f_t + f_r, b_t) - \min(f_t, b_t - b_r))}$$

We then employ the Hopcroft-Karp-Karzanov algorithm Hopcroft and Karp [1973] to compute the maximum weighted matching, M , where each edge must have weight exceeding a threshold (which is set on the validation set, see Section 5). For each element

$$((f_t, f_d, f_r, f_c), (b_t, b_d, b_r, b_c)) \in M,$$

we form a combined prediction for a bounding box from f_t to b_t , with prediction probability $1 - (1 - f_d)(1 - b_d) \text{ioU}_{f,b}$, where $\text{ioU}_{f,b}$ is the IoU between events f and b . The class probability is taken from the forward prediction. We also include all the bounding boxes predicted by the forward and backward predictions that were not part of the matching. Thus, our final set of predicted bounding boxes, each of the form (onset time, offset time, detection probability, class probability) is

$$\begin{aligned} P = & \{(f_t, b_t, 1 - (1 - f_d)(1 - b_d), f_c) | \\ & ((f_t, f_d, f_r, f_c), (b_t, b_d, b_r, b_c)) \in M\} \\ & \cup \{(f_t, f_t + f_r, f_d, f_c) | (f_t, f_d, f_r, f_c) \in F'\} \\ & \cup \{(b_t, b_t + b_r, b_d, b_c) | (b_t, b_d, b_r, b_c) \in B'\}, \end{aligned}$$

where F' and B' are, respectively, the forward and backward predictions that were not matched. We then select all predictions whose probability is greater than a threshold. The bidirectional method is illustrated in Figure 2.

4 Overlapping Zebra Finch Dataset (OZF)

We release a new dataset, OZF, specifically focused on overlapping vocalizations. OZF consists of a real-world portion of live recordings and synthetic portion in which we combined samples to exactly control the degree of overlap.

4.1 OZF Real-World Portion

We recorded 65 minutes (divided into 60-second files) of female ZFs. Eight adult (> 1 year) female ZFs were housed in a large group cage in a sound attenuating chamber (TRA Acoustics, Ontario, Canada). We continuously recorded using Audacity (3.3.3) through two omnidirectional microphones (Countryman, Menlo Park, CA) positioned above and to the side of the cage. Food and water were provided *ad libitum* and all procedures were approved by the University’s Animal Care and Use Committee in accordance with the guidelines of the Canadian Council on Animal Care.

Female ZFs make short, discrete vocalizations of about 100ms, consisting of a flat or downward sweeping harmonic stack, with most energy located between 0.5 and 8 kHz (Figure 1) Zann [1996], Ter Maat et al. [2014]. The recordings were divided among three annotators, who marked the onset and offset time of each vocalization using Raven Pro (Cornell Lab of Ornithology, v.1.6.5). Annotators covered 25 minutes each. One 5 minute section was annotated by all three, where the mean pairwise inter-annotator agreement was 93.5 F1@0.5IoU. We also computed agreement on the subset of vocalizations that overlapped as 78.1 F1@0.5IoU. Although the released audio data is mono, annotators used stereo tracks to improve accuracy.

Out of a total of 8504 vocalizations in the dataset, 1449 (17.04%) overlap with at least one other vocalization. The total number of overlaps is slightly higher at 1463, as some vocalizations can overlap two others. The number of vocalizations per 60 s file ranges from 19 to 245, while the number overlapping ranges from 0 to 73. We observe an approximately linear relationship between the two. The duration of each vocalization ranges from 3 ms to 350 ms and is strongly peaked around the mean of 109 ms (Figure 3). Further summaries are contained in the Appendix.

In Appendix B, we show that, assuming independent vocalizations from each bird that can be modelled with a Poisson distribution, the expected number of pairwise overlaps is

$$d(n-1) \left(1 - \frac{1}{B} - \frac{1}{n} \right), \quad (1)$$

where d is the ratio of total call durations to time window size, n is the number of vocalizations and B is the number of birds. In our case, $B = 8$, $n \approx 120$ and $d \approx 0.1$. Plugging the values for n and d from each 60 s file into (1), the average ratio of overlap to number of vocalizations should be 20.46%. The overlap of 17% is below what would be expected under these modelling assumptions, and the difference is highly significant (shown in Appendix B). This is consistent with prior work showing evidence for turn-taking in female ZFs Benichov et al. [2016].

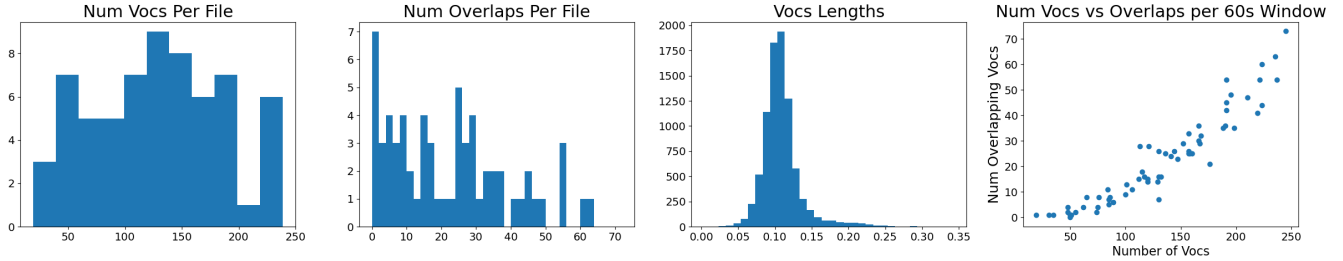


Figure 3: Summary of the live portion of the dataset we release. Left: number of vocalizations per 60 s file. Second: number of overlapping pairs per 60 s file. Third: distribution of the lengths of vocalizations. Right: number of vocalizations per 60 s file vs number overlapping pairs.

4.2 OZF Synthetic Portion

In addition to the real-world portion of our OZF dataset, we generate six synthetic ZF datasets where in each 60-second file, the ratio overlaps to number of calls is controlled. The synthetic dataset is constructed by adding cropped denoised female ZF vocalizations, drawn randomly from a call database (Appendix A.2), to a background track. The background tracks were also recorded using the same setup as the OZF dataset, but were filtered to contain no vocalizations.

To construct one synthetic dataset, we fix a target overlap-to-call ratio

$$R \in \{0.0, 0.2, 0.4, 0.6, 0.8, 1.0\}.$$

There are 65 recordings in each synthetic dataset. Each recording mimics one 60-second source recording in OZF, has the same number of vocalizations as the source recording and is placed in the same train/val/test split. To construct one synthetic recording, we count the number of calls present in the OZF source recording and randomly draw an equal number from the call database, and add them sequentially to the background track. When the current overlap-to-call ratio is below the target R , the next call is placed to overlap an existing call; otherwise, it is placed to not overlap. When $R > 0.2$, the first 25% of calls are placed uniformly at random to reduce clumping of calls around one point. Each of the six synthetic datasets ends up with an average a overlap-to-call ratio of within 0.005 of the target R . Call amplitude is chosen so that signal-to-noise ratio falls uniformly at random between -15dB and 0dB.

5 Experimental Evaluation

Implementation Details We first extract features from the raw audio using a backbone encoder, and then make the predictions described in Section 3 from the extracted features. The encoder converts input audio (mono, 16 kHz) to a frame-based representation, which is a sequence of latent vectors produced at 50 Hz. For the main experiments, we use BEATS Chen et al. [2023] as a backbone encoder. BEATS is an encoder-only transformer, consisting of 12 layers with hidden size 768 and 8 attention heads, pretrained on Audioset Gemmeke et al. [2017]. In Section 5.2, we explore different choices of backbone. The detection, regression and classification predictions are then each made using a linear layer. The loss function hyperparameters were fixed at $\alpha = 2$, $\beta = 4$, and $\sigma = 6$. Training lasts for 50 epochs, with the encoder frozen for the first 3 epochs. We use Adam with ams-grad, $\beta_1 = 0.9$, $\beta_2 = 0.999$, and a cosine annealing scheduler. For all models, we try three base learning rates, $1e-4$, $3e-5$ and $1e-5$, and select the one with the best mean average precision @0.5IoU on the val set. For F1, the bidirectional matching threshold is fit to F1@0.8 on the val set. We apply soft non-maximal suppression Bodla et al. [2017] with $\sigma = 0.5$.

Datasets In addition to our newly released OZF dataset, we evaluated Voxaboxen using seven existing strongly-labelled bioacoustics datasets. These datasets were selected for their taxonomic diversity, and include sounds made by amphibians (AnuraSet), insects (Katydid), birds (BirdVox-10h, Hawaiian Birds, Powdermill), and mammals (Humpback, Meerkat). Details for each dataset are given in Table 1. The list of the preprocessing steps we performed on these datasets is in Appendix C. For Katy, BV10 and OZF, the events of interest were brief and, for Katy and BV10, often above the 8kHz Nyquist frequency assumed by several of the models we evaluated. For all models, we use a half-time version of BV10 and OZF, and a one-sixth time version of Katy. Initial experiments indicated that using these slowed-down versions dramatically improved performance.

Dataset	Num files	Num classes	Dur. (hr)	Num events	Mean event dur. (sec)	Overlap Ratio	Recording type	Location	Taxa
Anuraset (AnSet) Cañas et al. [2023]	1612	10	26.82	7807	6.23	13.8%	TPAM	Brazil	Anura
BirdVox-10h (BV10) Nolasco et al. [2023]	15	1	10.00	9024	0.15	10.04%	TPAM	New York, USA	Passeriformes
Hawaii Birds (HawB) Navine et al. [2022]	635	9	50.88	55713	1.11	11.01%	TPAM	Hawaii, USA	Aves
Humpback (HbW) Allen et al. [2021]	642	1	13.38	4776	0.99	4.59%	UPAM	North Pacific Ocean	Megaptera novaeangliae
Katydid (Katy) Madhusudhana et al. [2024]	27	1	4.49	11961	0.17	7.88%	TPAM	Panamá	Tettigoniidae
Meerkat (MT) Nolasco et al. [2023]	6	1	1.26	1294	0.15	0.08%	On-body	South Africa	Suricata suricatta
Powdermill (Pow) Chronister et al. [2021]	77	6	6.42	9919	1.11	5.59%	TPAM	Pennsylvania, USA	Passeriformes
Overlapping Zebra Finch (OZF)	65	1	1.08	8504	0.11	17.04%	Laboratory	Laboratory	Taeniopygia castanotis

Table 1: Summary of datasets used to evaluate model performance. Terrestrial and underwater passive acoustic monitoring units are abbreviated as TPAM and UPAM, respectively.

Metrics We report F1 score and mean average precision (mAP). For F1, we fix the detection threshold to 0.5. A detection threshold is not required for mAP. Instead it sweeps a range of thresholds to obtain a range of precision and recall scores, and then calculates the average precision across equally-sized intervals of recall score. We compute mAP as proposed in Everingham et al. [2010], except using 1001 equally-sized intervals rather than 11. Before computing both metrics, we compute a matching between predicted events and ground truth events. We follow Nolasco et al. [2023] in using the Hopcroft-Karp-Karzanov algorithm, and only counting matches that exceed a certain IoU threshold. We report results for an IoU threshold of 0.5 and of 0.8.

Comparison Models We compare the performance of `Voxaboxen` to two existing object detection models and four frame-based SED methods. For the former, we use Faster-RCNN Ren et al. [2016], from the public available implementation², with the X-101 model checkpoint, pre-trained on MS COCO Lin et al. [2014]. We also use the model of Ye et al. [2021], an encoder-decoder transformer, adapted to detect 1d events from a spectrogram.

For the latter, we train a linear layer on top of three pre-trained encoder-only transformers, to predict the presence or absence of each class in each frame. The encoders are Frame-ATST Shao et al. [2024] (25 Hz, pretrained on Audioset), BEATS Chen et al. [2023] (50 Hz, pretrained on Audioset) and BirdAVES Hagiwara [2023]³ (50 Hz, pre-trained on animal sound datasets). Output are median filtered, with kernel size 1, 3, 7, or 11, selected from val set performance.

We also compare to a randomly initialized convolutional-recurrent neural network (CRNN) Cakir et al. [2017], Cohen et al. [2022], Martin et al. [2022]. operating on log mel-spectrograms, comprising a 2d conv layer with kernel size 7, and hidden size 64, mean-pooling in the frequency dimension, with kernel size 2, two 2d residual blocks He et al. [2016] with kernel size 3, mean pooling in both directions with kernel size 2, and finally a bidirectional LSTM Hochreiter and Schmidhuber [1997], with hidden size 1024.

In our synthetic dataset experiments, we implement a source-separate baseline on top of a frame-based detection method. We separate audio into four tracks using the pre-trained BirdMixIT model Denton et al. [2022], and feed it into a frame-based detector fine-tuned on the original (non-separated) data. We combine the four sets of detections

²<https://github.com/facebookresearch/detectron2>

³<https://github.com/earthspecies/aves>

Metric	Method	AnSet	BV10	HawB	HbW	Katy	MT	Pow	OZF
mAP@0.5IoU	CRNN	9.89	35.59	22.72	21.03	17.24	82.97	35.45	71.80
	Faster-RCNN	8.06	55.49	7.39	21.66	25.93	84.22	14.08	90.20
	DETR	0.18	3.79	2.79	3.95	2.30	18.58	2.71	2.26
	Frame-ATST	14.87	40.62	32.19	33.62	17.88	87.58	45.42	73.48
	BEATS	15.71	48.01	35.37	37.13	20.12	86.08	50.32	77.94
	BirdAVES	14.21	42.09	32.67	26.54	19.11	86.11	43.52	78.33
	Voxaboxen (Ours)	24.24	77.58	57.37	57.58	36.87	90.85	50.91	97.92
mAP@0.8IoU	CRNN	2.43	12.96	5.04	3.39	1.90	37.10	16.54	30.05
	Faster-RCNN	3.43	29.08	2.24	3.03	9.53	53.54	9.09	69.06
	DETR	0.16	0.18	0.12	0.10	0.11	0.13	0.16	0.10
	Frame-ATST	4.72	18.20	10.55	8.28	2.66	24.70	23.44	27.11
	BEATS	5.18	18.98	10.31	9.77	2.93	51.00	27.11	42.27
	BirdAVES	4.52	19.28	9.12	5.14	3.08	48.29	23.04	42.44
	Voxaboxen (Ours)	9.31	36.89	22.05	21.15	8.75	65.80	31.30	81.23
F1@0.5IoU	CRNN	19.93	54.36	38.33	42.93	33.20	87.39	47.75	80.00
	Faster-RCNN	16.57	64.60	13.44	34.15	33.63	90.08	25.94	92.77
	DETR	0.50	18.60	11.93	15.54	14.22	38.51	9.19	14.35
	Frame-ATST	27.69	60.35	51.14	54.14	25.01	89.30	56.76	81.09
	BEATS	30.24	63.86	52.58	58.46	31.06	87.85	61.48	84.83
	BirdAVES	26.11	60.31	52.23	49.97	32.05	86.07	54.86	85.56
	Voxaboxen (Ours)	25.72	74.12	59.53	61.23	38.12	88.17	56.67	95.73
F1@0.8IoU	CRNN	9.54	33.69	17.61	16.28	11.43	40.33	31.62	52.58
	Faster-RCNN	9.41	46.38	7.37	11.69	18.91	71.83	19.95	80.90
	DETR	0.01	1.46	0.74	0.93	0.13	1.72	0.73	0.22
	Frame-ATST	13.56	40.48	28.02	25.46	12.17	24.70	38.77	48.83
	BEATS	15.67	41.53	27.96	28.09	11.43	71.64	44.02	64.66
	BirdAVES	13.06	41.50	26.74	21.40	11.61	66.53	38.73	64.49
	Voxaboxen (Ours)	14.68	54.07	35.96	36.85	19.27	75.70	42.30	84.46

Table 2: F1 and mean average precision scores at 0.5 and 0.8 IoU. Best results in **bold**. With a handful of exceptions, Voxaboxen outperforms existing methods, and is sometimes far ahead, for example on BV10 and OZF.

and apply soft non-maximal suppression to de-duplicate boxes. Based on performance on the live OZF dataset, we use BirdAVES as our frame-based detector for synthetic datasets.

The training parameters and hyper-parameter search is the same as that of Voxaboxen for all baselines.

5.1 Main Results

As shown in Table 2, Voxaboxen outperforms all baselines on almost all datasets and metrics. The few occasions where it does not are mAP@0.8 on Katy, F1@0.5 on MT, both F1’s on AnSet, and F1@0.8 on Pow. In several cases, Voxaboxen is far ahead of all other models, e.g. 10+ points on mAP@0.5 on BV10, HawB, HbW, and Katy. At mAP@0.8, Voxaboxen scores 5+ points ahead of others on BV10, HawB, HbW, MT, and OZF. The diversity of animal sounds in the datasets especially highlights the general effectiveness of our method.

The Faster-RCNN generally performs well on OZF and MT, and slightly surpasses Voxaboxen on Katy mAP@0.8. However, it struggles with datasets with more than one class (AnSet, HawB, and Pow), as well as HbW. Of the frame-level SED models, Frame-ATST, BEATS and BirdAVES, BEATS is generally the strongest, which is consistent with our findings for the backbone choice in Voxaboxen (see Table 3).

The DETR model from Ye et al. [2021] is poor. The model has been pretrained on datasets mostly of ambient city noises, and transfers badly to animal vocalizations. We used the authors’ public code and tried all available pretrained checkpoints. We also contacted the authors to ask about additional data preprocessing, and received no response.

Metric	Method	AnSet	BV10	HawB	HbW	Katy	MT	Pow	OZF
mAP@0.5IoU	Voxaboxen (main)	24.24	80.67	57.37	57.58	36.05	91.12	50.91	97.92
	Voxaboxen with BirdAVES encoder	22.86	46.33	49.22	48.04	26.59	88.78	50.21	96.36
	Voxaboxen no fwd-bck matching	23.76	78.75	49.20	56.41	30.44	90.90	48.41	95.77
mAP@0.8IoU	Voxaboxen (main)	9.31	42.65	22.05	21.15	8.54	65.80	31.30	81.23
	Voxaboxen w/ BirdAVES encoder	8.64	25.56	18.55	12.22	5.16	56.31	32.31	74.32
	Voxaboxen no fwd-bck matching	8.43	40.30	14.59	18.01	5.37	43.18	26.17	80.36

Table 3: Ablation studies on the backbone encoder and the forward-backward matching method. The main model uses the BEATS encoder. Best results in **bold**. Both ablation settings give a moderate, consistent drop in performance, showing the superiority of the BEATS encoder over BirdAVES, and the effectiveness of the Voxaboxen forward-backward matching method.

Metric	Method	0.0	0.2	0.4	0.6	0.8	1.0	OZF
mAP@0.5IoU	Faster-RCNN	98.54	91.95	87.63	83.87	80.33	75.63	90.20
	BirdAVES	98.66	81.19	62.74	52.60	38.88	29.76	78.33
	BirdAVES + BirdMixIT	85.92	59.83	52.05	41.79	34.78	26.63	66.96
	Voxaboxen (Ours)	99.85	98.19	97.23	95.93	94.17	92.77	97.72
mAP@0.8IoU	Faster-RCNN	96.96	87.92	81.87	78.30	73.09	68.10	69.06
	BirdAVES	92.72	63.41	39.82	28.46	17.85	11.58	42.44
	BirdAVES + BirdMixIT	77.42	43.77	30.91	21.20	13.55	8.66	30.40
	Voxaboxen (Ours)	98.95	95.80	93.62	90.64	88.16	83.19	81.23

Table 4: F1 and mean average precision on the synthetic portion of our OZF dataset, which comes in six varieties with increasing overlap. Columns show number of overlaps / number of total vox. Last column is the natural portion of OZF, which has overlap ratio = 0.174. Best results in **bold**. Existing methods, especially the frame-based BirdAVES and BirdAVES + BirdMixIT, deteriorate as the overlap ratio increases. Voxaboxen is consistently the most accurate and drops only slightly with increasing overlap.

5.2 Ablation Studies

Table 3 shows the effect of changing the encoder backbone of Voxaboxen, and of removing the forward-backward matching procedure. We found that using BirdAVES as a backbone for Voxaboxen reduced performance compared with the version of that used the BEATS encoder. This was surprising considering BirdAVES was designed specifically for animal sounds; however differences in pre-training data volume and training regimes may explain the performance difference. Removing forward-backward matching also consistently lowers the mAP scores. Mostly the difference is 1-2 points but larger for some datasets, e.g. HawB and Katy.

5.3 Performance on OZF-synthetic

Table 4 shows the performance of Voxaboxen on the synthetic portion of our newly-released OZF dataset. The leftmost column shows the synthetic dataset version with no overlaps (ratio=0), and this increases from left to right, until the version with the ratio=1, where the number of pairwise overlaps equals the total number of vocalizations. Voxaboxen outperforms the comparison models at all overlap ratios, and maintains a high accuracy (92.77 mAP@0.5, 83.19 mAP@0.8), even at the highest over ratio of 1. BirdAVES, with and without BirdMixIT, deteriorates sharply with increasing overlap ratio, consistent with our argument that frame-based methods are insufficient for handling overlapping vocalizations. FasterRCNN fares better than other baselines, but is still firmly behind Voxaboxen.

6 Conclusion

In this work, we introduced Voxaboxen, a novel method for sound event detection in bioacoustic recordings, specifically designed to address the challenges posed by overlapping vocalizations. Voxaboxen uses bidirectional predictions of vocalization boundaries combined with a graph-matching algorithm to accurately identify and localize events. To advance evaluation of overlapping vocalization detection, we released a new dataset, OZF, of zebra finch record-

ings with temporally-strong annotations and frequent overlaps. Extensive testing on seven existing datasets and our new dataset demonstrates that `Voxaboxen` achieves state-of-the-art performance, with particularly notable improvements over standard SED methods in scenarios with high overlap. This work highlights the potential of `Voxaboxen` to advance bioacoustic research in ethology, ecology, and conservation.

References

- Sharath Adavanne, Archontis Politis, Joonas Nikunen, and Tuomas Virtanen. Sound event localization and detection of overlapping sources using convolutional recurrent neural networks. *IEEE J. Sel. Top. Signal Process.*, 13(1), 2018.
- Mohammed Algabri, Hassan Mathkour, et al. Towards deep object detection techniques for phoneme recognition. *IEEE Access*, 8, 2020.
- Ann N. Allen, Matt Harvey, Lauren Harrell, Aren Jansen, et al. A convolutional neural network for automated detection of humpback whale song in a diverse, long-term passive acoustic dataset. *Front. Mar. Sci.*, 8, 2021. ISSN 2296-7745. doi: 10.3389/fmars.2021.607321. URL <https://www.frontiersin.org/journals/marine-science/articles/10.3389/fmars.2021.607321>.
- Thierry Aubin and Pierre Jouventin. How to vocally identify kin in a crowd: The penguin model. In *Advances in the Study of Behavior*, Advances in the study of behavior. 2002.
- Jonathan I Benichov, Sam E Benezra, Daniela Vallentin, Eitan Globerson, Michael A Long, and Ofer Tchernichovski. The forebrain song system mediates predictive call timing in and male zebra finches. *Curr. Biol.*, 26(3), 2016.
- Peter C Bermant. Biocppnet: automatic bioacoustic source separation with deep neural networks. *Sci. Rep.*, 11(1), 2021.
- Victor Bisot, Slim Essid, and Gaël Richard. Overlapping sound event detection with supervised nonnegative matrix factorization. In *ICASSP*, 2017.
- Navaneeth Bodla, Bharat Singh, Rama Chellappa, and Larry S Davis. Soft-nms—improving object detection with one line of code. In *CVPR*, 2017.
- Hervé Bredin and Antoine Laurent. End-to-end speaker segmentation for overlap-aware resegmentation. In *Interspeech*, 2021. doi: 10.21437/Interspeech.2021-560.
- Emre Cakir, Giambattista Parascandolo, Toni Heittola, Heikki Huttunen, et al. Convolutional recurrent neural networks for polyphonic sound event detection. *IEEE/ACM Trans. Audio Speech Lang. Process.*, 25(6), 2017. ISSN 2329-9290. doi: 10.1109/TASLP.2017.2690575. URL <https://doi.org/10.1109/TASLP.2017.2690575>.
- María Cañas, Juan Toro-Gómez, Larissa Sayuri Moreira Sugai, et al. A dataset for benchmarking neotropical anuran calls identification in passive acoustic monitoring. *Sci. Data*, 10(1), 2023.
- Nicolas Carion, Francisco Massa, Gabriel Synnaeve, Nicolas Usunier, Alexander Kirillov, and Sergey Zagoruyko. End-to-end object detection with transformers. In *ECCV*, 2020.
- Sanyuan Chen, Yu Wu, Chengyi Wang, Shujie Liu, Daniel Tompkins, Zhuo Chen, and Furu Wei. Beats: Audio pre-training with acoustic tokenizers. In *ICML*, 2023. URL <https://www.microsoft.com/en-us/research/publication/beats-audio-pre-training-with-acoustic-tokenizers/>.
- Lauren M. Chronister, Tessa A. Rhinehart, Aidan Place, and Justin Kitzes. An annotated set of audio recordings of eastern north american birds containing frequency, time, and species information. *Ecology*, 102(6):e03329, 2021.
- Simon Clulow, Michael Mahony, Lang Elliott, Sarah Humfeld, and H Carl Gerhardt. Near-synchronous calling in the hip-pocket frog *assa darlingtoni*. *Bioac.*, 26(3), 2017.

- Yarden Cohen, David Aaron Nicholson, Alexa Sanchioni, Emily K Mallaber, et al. Automated annotation of birdsong with a neural network that segments spectrograms. *eLife*, 11, 2022. ISSN 2050-084X. doi: 10.7554/eLife.63853. URL <https://doi.org/10.7554/eLife.63853>.
- Tom Denton, Scott Wisdom, and John R Hershey. Improving bird classification with unsupervised sound separation. In *ICASSP*, 2022.
- Arnaud Dessein, Arshia Cont, and Guillaume Lemaitre. Real-time detection of overlapping sound events with non-negative matrix factorization. *Matrix Inf. Geom.*, 2013.
- Janek Ebbers, Francois G Germain, Gordon Wichern, and Jonathan Le Roux. Sound event bounding boxes. In *Interspeech*, 2024. doi: 10.21437/Interspeech.2024-2075.
- Julie E Elie, Hédi A Soula, Nicolas Mathevon, and Clémentine Vignal. Dynamics of communal vocalizations in a social songbird, the zebra finch (*taeniopygia guttata*). *JASA*, 129(6), 2011.
- Mark Everingham, Luc Van Gool, Christopher KI Williams, John Winn, and Andrew Zisserman. The pascal visual object classes (voc) challenge. *Int. J. Comput. Vis.*, 88, 2010.
- Lauren Fitzsimmons, Jennifer Foote, Laurene Ratcliffe, and Daniel Mennill. Frequency matching, overlapping and movement behaviour in diurnal countersinging interactions of black-capped chickadees. *Anim. Behav.*, 75(6), 2008.
- Jort F Gemmeke, Daniel PW Ellis, Dylan Freedman, Aren Jansen, Wade Lawrence, R Channing Moore, Manoj Plakal, and Marvin Ritter. Audio set: An ontology and human-labeled dataset for audio events. In *ICASSP*, 2017.
- Erin Gillam and M. Brock Fenton. *Roles of Acoustic Social Communication in the Lives of Bats*. New York, NY, 2016. ISBN 978-1-4939-3527-7. doi: 10.1007/978-1-4939-3527-7_5. URL https://doi.org/10.1007/978-1-4939-3527-7_5.
- Masato Hagiwara. Aves: Animal vocalization encoder based on self-supervision. In *ICASSP*, 2023. doi: 10.1109/ICASSP49357.2023.10095642.
- Fred H Harrington, Cheryl S Asa, L Mech, and L Boitani. Wolf communication. *Wolves Behav. Ecol. Conserv.*, 3, 2003.
- Kaiming He, Xiangyu Zhang, Shaoqing Ren, and Jian Sun. Deep residual learning for image recognition. In *CVPR*, 2016.
- Sepp Hochreiter and Jürgen Schmidhuber. Long short-term memory. *Neural Comput.*, 9(8), 1997. ISSN 0899-7667. doi: 10.1162/neco.1997.9.8.1735. URL <https://doi.org/10.1162/neco.1997.9.8.1735>.
- John E Hopcroft and Richard M Karp. An $n^{5/2}$ algorithm for maximum matchings in bipartite graphs. *SIAM J. Comput.*, 2(4), 1973.
- Stefan Kahl, Connor M. Wood, Maximilian Eibl, and Holger Klinck. Birdnet: A deep learning solution for avian diversity monitoring. *Ecol. Inform.*, 61, 2021. ISSN 1574-9541. doi: <https://doi.org/10.1016/j.ecoinf.2021.101236>. URL <https://www.sciencedirect.com/science/article/pii/S1574954121000273>.
- Arik Kershenbaum, Daniel T Blumstein, Marie A Roch, et al. Acoustic sequences in non-human animals: a tutorial review and prospectus. *Biol. Rev. Camb. Philos. Soc.*, 91(1), 2016.
- Paola Laiolo. The emerging significance of bioacoustics in animal species conservation. *Bio. Cons.*, 143(7), 2010.
- Luke C Larter and Michael J Ryan. Female preferences for more elaborate signals are an emergent outcome of male chorusing interactions in túngara frogs. *American Naturalist*, 203(1), 2024.
- Hei Law and Jia Deng. Cornernet: Detecting objects as paired keypoints. In *ECCV*, 2018.
- Henry D Legett, Rachel A Page, and Ximena E Bernal. Synchronized mating signals in a communication network: the challenge of avoiding predators while attracting mates. *Trans. Roy. Soc. B*, 286(1912), 2019.

- Henry D Legett, Ikkyu Aihara, and X E Bernal. The dual benefits of synchronized mating signals in a japanese treefrog: attracting mates and manipulating predators. *Transa. Roy. Soc. B*, 376(1835), 2021.
- Tsung-Yi Lin, Michael Maire, Serge Belongie, James Hays, Pietro Perona, Deva Ramanan, Piotr Dollár, and C Lawrence Zitnick. Microsoft coco: Common objects in context. In *ECCV*, 2014.
- Shyam Madhusudhana, Holger Klinck, and Laurel B Symes. Extensive data engineering to the rescue: building a multi-species katydid detector from unbalanced, atypical training datasets. *Trans. of the Roy. Soc. B*, 379(1904), 2024.
- Killian Martin, Olivier Adam, Nicolas Obin, and ValÉ©rie Dufour. Rookognise: Acoustic detection and identification of individual rooks in field recordings using multi-task neural networks. *Ecol. Inform.*, 72, 2022. ISSN 1574-9541. doi: <https://doi.org/10.1016/j.ecoinf.2022.101818>. URL <https://www.sciencedirect.com/science/article/pii/S1574954122002680>.
- Amanda Navine, Stefan Kahl, Ann Tanimoto-Johnson, Holger Klinck, and Patrick Hart. A collection of fully-annotated soundscape recordings from the island of hawai'i, 2022. URL <https://doi.org/10.5281/zenodo.7078499>.
- Ines Nolasco, Shubhr Singh, Veronica Morfi, Vincent Lostanlen, et al. Learning to detect an animal sound from five examples. *Ecol. Inform.*, 77, 2023.
- Karan J Odom, Marcelo Araya-Salas, Janelle L Morano, Russell A Ligon, et al. Comparative bioacoustics: a roadmap for quantifying and comparing animal sounds across diverse taxa. *Biological Review Cambridge Phil. Soc.*, 96(4), 2021.
- Weronika Penar, Angelika Magiera, and Czesław Klocek. Applications of bioacoustics in animal ecology. *Ecol. Compl.*, 43(100847), 2020.
- Shaoqing Ren, Kaiming He, Ross Girshick, and Jian Sun. Faster r-cnn: Towards real-time object detection with region proposal networks. *IEEE Trans. Pattern Anal. Mach. Intell.*, 39(6), 2016.
- Tyler M Schulz, Hal Whitehead, Shane Gero, and Luke Rendell. Overlapping and matching of codas in vocal interactions between sperm whales: insights into communication function. *Anim. Behav.*, 76(6), 2008.
- Nian Shao, Xian Li, and Xiaofei Li. Fine-tune the pretrained atst model for sound event detection. In *ICASSP*, 2024. doi: 10.1109/ICASSP48485.2024.10446159.
- Kazuki Shimada, Yuichiro Koyama, Shusuke Takahashi, Naoya Takahashi, et al. Multi-accdoa: Localizing and detecting overlapping sounds from the same class with auxiliary duplicating permutation invariant training. In *ICASSP*, 2022.
- Joseph Soltis, Kirsten Leong, and Anne Savage. African elephant vocal communication i: antiphonal calling behaviour among affiliated females. *Anim. Behav.*, 70(3), 2005.
- Dan Stowell. Computational bioacoustics with deep learning: a review and roadmap. *PeerJ*, 2022. doi: 10.7717/peerj.13152.
- Dan Stowell, Tereza Petrusková, Martin Šálek, and Pavel Linhart. Automatic acoustic identification of individuals in multiple species: improving identification across recording conditions. *J. of the Roy. Soc. Interface*, 16(153), 2019.
- Andries Ter Maat, Lisa Trost, Hannes Sagunsky, Susanne Selmann, and Manfred Gahr. Zebra finch mates use their forebrain song system in unlearned call communication. *PLoS One*, 9(10), 2014.
- Zhirong Ye, Xiangdong Wang, Hong Liu, Yueliang Qian, et al. Sound event detection transformer: An event-based end-to-end model for sound event detection. *arXiv preprint arXiv:2110.02011*, 2021.
- Tomoya Yoshinaga, Keitaro Tanaka, Yoshiaki Bando, Keisuke Imoto, and Shigeo Morishima. Onset-and-offset-aware sound event detection via differentiable frame-to-event mapping. *IEEE Signal Process. Lett.*, 32, 2025. doi: 10.1109/LSP.2024.3509336.

Richard A Zann. *The zebra finch: a synthesis of field and laboratory studies*. 1996.

Sándor Zsebők, Máté Ferenc Nagy-Egri, Gergely Gábor Barnaföldi, Miklós Laczi, et al. Automatic bird song and syllable segmentation with an open-source deep-learning object detection method—a case study in the collared flycatcher. *Ornis Hung.*, 27(2), 2019.

A OZF Further Details

A.1 Segmentwise Statistics of the Real-World Portion

Figure 3 reported the distribution of vocalizations and overlaps across each 60-second audio file.

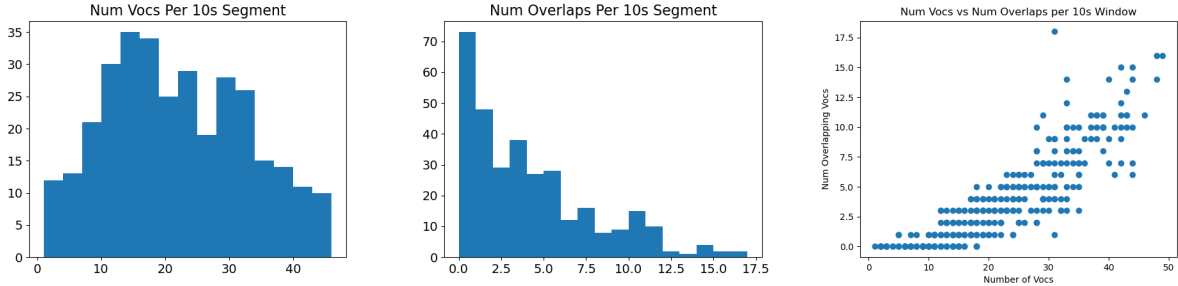


Figure 4: Statistics from the real-world portion of OZF, across 10 s segments. Top: the distribution of the number of vocalizations entirely contained within each 10 s segment, across all audio files. Middle: the distribution of the number of pairwise overlaps of these vocalizations. Bottom: the number of vocalizations vs the number of pairwise overlaps across each 10 s segment.

A.2 Call Database for the Synthetic Portion

To construct the synthetic datasets, we created a database of female ZF calls. To construct this, female ZFs were recorded using the same setup as with the live portion of OZF. Calls were detected using an initial version of `Voxaboxen`, and cropped versions of the calls were saved. We then performed a denoising procedure: First, using `BirdMixit` Denton et al. [2022] each of these cropped calls was separated into four stems. Then, our trained model was again run across each of these four stems, and we retained a stem when `Voxaboxen` both 1) detected a call and 2) the model detection confidence was higher on this stem than the other three stems. Finally, we observed that even after these steps there remained stems that contained no zebra finch vocalizations. To remove these, we performed a quality-filtering step: for each stem, we predicted the species of the call using `BirdNET` Kahl et al. [2021]. We retained only stems where `BirdNET` predicted a species with British English common name containing the word “Finch”. The stems that passed this quality filter became the database of denoised female zebra finch calls.

B Expected Number of Overlaps from Independent Memoryless Sources

Given a window of time and some set V of vocalizations whose onsets occur during this window, we are interested in the expected value of the number of pairs that overlap, assuming that the probability density function for the point of each onset is uniform and independent. Let L be the length of the time window, 60s in our case, so that the pdf equals $\frac{1}{L}$. Then, for any two vocalizations with onsets as v_1 and v_2 of respective durations l_1 and l_2 , the probability of overlap is

$$\frac{l_1 + l_2}{L}, \quad (2)$$

because they will overlap if and only if v_1 falls in the interval $(v_2 - l_1, v_2 + l_1)$, which is of length $l_1 + l_2$.

The expected number of overlaps, $\mathbb{E}[X]$, is the sum, across all ordered pairs of vocalizations, of the the indicator random variable for the event that they overlap, which equals the probability as given in (2). Let $|V| = n$, and let l_i

be the duration of the i vocalization, then

$$\begin{aligned}
 \mathbb{E}[X] &= \sum_{i=1}^n \sum_{j=1}^{i-1} \frac{l_i + l_j}{L} = \frac{1}{L} \left(\sum_{i=1}^n \sum_{j=1}^{i-1} l_i + l_j \right) \\
 &= \frac{1}{L} \left(\sum_{i=1}^n (i-1)l_i + \sum_{i=1}^n \sum_{j=1}^i l_j \right) \\
 &= \frac{1}{L} \left(\sum_{i=1}^n (i-1)l_i + \sum_{j=1}^{n-1} \sum_{i=j}^n l_j \right) \\
 &= \frac{1}{L} \left(\sum_{i=1}^n (i-1)l_i + \sum_{j=1}^{n-1} (n-j)l_j \right) \\
 &= \frac{1}{L} \left(\sum_{i=1}^n (i-1)l_i + \sum_{i=1}^{n-1} (n-i)l_i \right) \\
 &= \frac{1}{L} \left(\sum_{i=1}^n (i-1)l_i + \sum_{i=1}^n (n-i)l_i \right) \\
 &= \frac{1}{L} \left(\sum_{i=1}^n (i-1)l_i + (n-i)l_i \right) \\
 &= \frac{1}{L} \left(\sum_{i=1}^n (n-1)l_i \right) \\
 &= (n-1) \frac{\sum_{i=1}^n l_i}{L}.
 \end{aligned}$$

Thus, we see that the expected number of overlaps for uniform independent vocalizations is the product of two factors. The first is the vocalization density

$$d = \frac{\sum_{i=1}^n l_i}{L}, \quad (3)$$

which is the ratio between the length of all vocalizations played back to back and the duration of the time window in which they occur, or equivalently, the expected number of vocalizations occurring at any one point. The second factor is the number of vocalizations (minus 1).

$$\mathbb{E}[X] = d(n-1), \quad (4)$$

where d is as in (3).

In the case of our released dataset, we must also account for the fact that there is a finite number of birds (eight), and overlaps can only occur between vocalizations from two different birds. For two given vocalizations, let S be the event that they come from different birds, which has probability

$$P(S) = 1 - \frac{\sum_{j=1}^B (\sum_{i=1}^n \mathbb{1}(b_i = j))^2}{n^2}, \quad (5)$$

where B is the number of birds and b_i is the bird that produced the i th vocalization. Let $Z_j = \sum_{i=1}^n \mathbb{1}(b_i = j)$ be the random variable counting the number of times the j th bird vocalises in a given time window (60s for our dataset). Assuming this distribution is the same for all birds, we can drop the subscript and just write Z . The expression in (5) is linear apart from the square on Z , so we have

$$\begin{aligned}
 P(S) &= 1 - \frac{\sum_{j=1}^B \mathbb{E}[Z^2]}{n^2} = 1 - \frac{B\mathbb{E}[Z^2]}{n^2} \\
 &= 1 - \frac{B(\mathbb{E}[Z]^2 + \text{Var}(Z))}{n^2}.
 \end{aligned}$$

If we model the vocalizations of each individual bird as a Poisson distribution, then we have

$$\mathbb{E}[Z] = \text{Var}(Z) = \lambda = \frac{n}{B},$$

giving

$$P(S) = 1 - \frac{B\left(\left(\frac{n}{B}\right)^2 + \frac{n}{B}\right)}{n^2} = 1 - \frac{\frac{n^2}{B} + n}{n^2} = 1 - \left(\frac{1}{B} + \frac{1}{n}\right).$$

The value from (4) is then the probability of overlap between two vocalizations given they come from separate birds: $\mathbb{E}[X|S] = d(n-1)$, and the total probability of overlap is then

$$\mathbb{E}[X] = \mathbb{E}[X|S]P(S) = d(n-1)\left(1 - \frac{1}{B} - \frac{1}{n}\right). \quad (6)$$

B.1 Difference Between Expected and Observed Overlaps

Table 5 shows the observed number of pairwise overlaps per file, compared with the expected number from (1). The former is consistently lower than the latter. Indeed, looking at the ‘difference’ column, we see it has mean 9.73, and standard deviation 9.05. We can model this difference as a normal distribution by the central limit theorem, as it is the sum of 8 independent samples from the distribution of a single bird. With 65 files, the estimated population standard deviation of this normal distribution is

$$\frac{9.05}{\sqrt{65-1}} = \frac{9.05}{8} = 1.13,$$

so the t -value is $\frac{9.73}{1.13} = 8.61$. This is highly significant, as the significance threshold for 64 degrees of freedom is 3.23 at 99.9% confidence.

C Evaluation Dataset Preprocessing

AnuraSet We used the portion of the frog call dataset presented in Cañas et al. [2023] that includes strong temporal annotations (onset, offset, and species label). We randomly assigned files into train, validation, and test sets with ratios 60%/20%/20%. For our purpose, we retained only annotations corresponding to the ten most commonly occurring species in the dataset.

BirdVox-10h We used the version of the BirdVox dataset presented in Nolasco et al. [2023]. We divided each recording into three segments: the first 60% was assigned to the train set, the next 20% was assigned to the validation set, and the final 20% was assigned to the test set. For our purpose, we merged all annotations (species labels for multiple passerine species) into a single class (vocalization).

Hawaiian Birds We used the dataset of Hawaiian soundscapes presented in Navine et al. [2022]. We randomly assigned files into train, validation, and test sets with ratios 60%/20%/20%. For our purpose, we retained only annotations corresponding to the nine most commonly occurring bird species in the dataset.

Humpback We used the “initial” audit portion of the dataset of humpback whale vocalizations presented in Allen et al. [2021], retaining only the 75-second clips containing at least one annotation. We randomly assigned these clips into train, validation, and test sets with ratios 60%/20%/20%. Finally, we retained only annotations corresponding to humpback whales, and discarded other annotations (e.g. ship noise).

Katydid We used the dataset of katydid calls presented in Madhusudhana et al. [2024]. We randomly assign files into train, validation, and test sets with ratios 60%/20%/20%. For our purpose, we merged all annotations (species labels) into a single class (katydid call).

Meerkat We used the dataset of on-body Meerkat recordings presented in Nolasco et al. [2023] (abbreviated as MT in *loc. cit.*). We divided each recording into three segments: the first 60% was assigned to the train set, the next 20% was assigned to the validation set, and the final 20% was assigned to the test set. For our purpose, we merged all annotations (vocalization type labels) into a single class (meerkat vocalization).

Powdermill We used the dataset of Northeastern United States soundscapes presented in Chronister et al. [2021]. We randomly assigned files into train, validation, and test sets with ratios 60%/20%/20%. For our purpose, we retained only annotations corresponding to the six most commonly occurring bird species in the dataset.

file	n	d	B	expected overlaps	observed overlaps	difference
0	106	0.19	8	16.94	11	5.94
1	117	0.22	8	21.80	16	5.80
2	157	0.29	8	39.17	25	14.17
3	191	0.36	8	59.25	42	17.25
4	195	0.36	8	60.76	48	12.76
5	221	0.38	8	73.36	54	19.36
6	51	0.08	8	3.59	1	2.59
7	160	0.30	8	41.91	25	16.91
8	223	0.37	8	71.97	44	27.97
9	19	0.03	8	0.48	1	-0.52
10	48	0.09	8	3.80	2	1.80
11	31	0.06	8	1.40	1	0.40
12	50	0.08	8	3.43	0	3.43
13	147	0.28	8	34.87	23	11.87
14	210	0.39	8	71.42	47	24.42
15	191	0.36	8	59.05	45	14.05
16	219	0.40	8	75.20	41	34.20
17	237	0.41	8	85.24	54	31.24
18	235	0.44	8	90.18	63	27.18
19	51	0.08	8	3.60	1	2.60
20	50	0.09	8	3.57	1	2.57
21	85	0.15	8	11.14	7	4.14
22	136	0.24	8	28.27	25	3.27
23	141	0.23	8	28.35	24	4.35
24	74	0.13	8	8.32	2	6.32
25	166	0.33	8	47.87	30	17.87
26	65	0.13	8	6.90	8	-1.10
27	223	0.39	8	74.50	60	14.50
28	168	0.31	8	45.60	32	13.60
29	158	0.29	8	39.44	25	14.44
30	120	0.20	8	20.36	15	5.36
31	84	0.16	8	11.16	11	0.16
32	245	0.46	8	97.64	73	24.64
33	191	0.37	8	60.43	54	6.43
34	75	0.11	8	7.21	4	3.21
35	130	0.26	8	28.77	7	21.77
36	130	0.23	8	25.50	26	-0.50
37	86	0.14	8	10.15	8	2.15
38	152	0.27	8	35.18	29	6.18
39	55	0.10	8	4.40	2	2.40
40	176	0.29	8	44.43	21	23.43
41	115	0.18	8	18.08	18	0.08
42	157	0.28	8	37.95	33	4.95
43	35	0.04	8	1.29	1	0.29
44	85	0.16	8	11.32	5	6.32
45	89	0.16	8	12.18	6	6.18
46	198	0.35	8	60.38	35	25.38
47	113	0.25	8	24.49	28	-3.51
48	112	0.22	8	20.79	15	5.79
49	101	0.18	8	15.48	13	2.48
50	157	0.29	8	38.71	26	12.71
51	144	0.26	8	31.71	26	5.71
52	62	0.13	8	6.76	4	2.76
53	167	0.32	8	46.38	29	17.38
54	120	0.23	8	23.86	14	9.86
55	76	0.15	8	9.99	8	1.99
56	190	0.33	8	53.87	36	17.87
57	130	0.20	8	22.82	16	6.82
58	166	0.36	8	51.14	36	15.14
59	121	0.25	8	26.36	28	-1.64
60	132	0.23	8	25.98	16	9.98
61	48	0.08	8	3.26	4	-0.74
62	100	0.19	8	16.00	9	7.00
63	129	0.23	8	25.27	14	11.27
64	188	0.34	8	55.06	35	20.06

Table 5: Comparison of the expected number of overlaps by equation 1 and the observed number of overlaps, by 60s file.